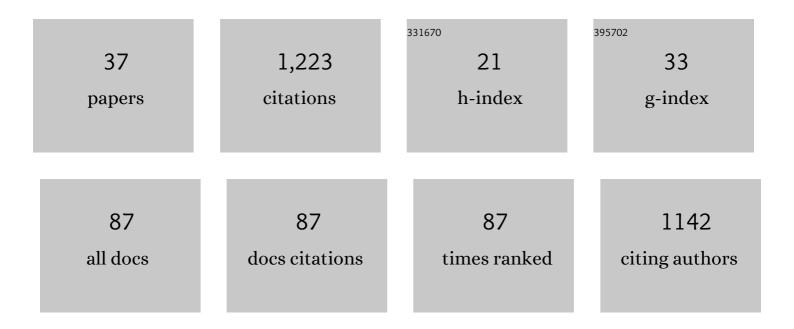


## List of Publications by Year in descending order

Source: https://exaly.com/author-pdf/1041744/publications.pdf Version: 2024-02-01



Προ ΕριεάΫ

#	Article	IF	CITATIONS
1	The Monte Carlo atmospheric radiative transfer model McArtim: Introduction and validation of Jacobians and 3D features. Journal of Quantitative Spectroscopy and Radiative Transfer, 2011, 112, 1119-1137.	2.3	174
2	MAX-DOAS formaldehyde slant column measurements during CINDI: intercomparison and analysis improvement. Atmospheric Measurement Techniques, 2013, 6, 167-185.	3.1	78
3	lodine monoxide in the Western Pacific marine boundary layer. Atmospheric Chemistry and Physics, 2013, 13, 3363-3378.	4.9	66
4	Cloud detection and classification based on MAX-DOAS observations. Atmospheric Measurement Techniques, 2014, 7, 1289-1320.	3.1	63
5	Intercomparison of aerosol extinction profiles retrieved from MAX-DOAS measurements. Atmospheric Measurement Techniques, 2016, 9, 3205-3222.	3.1	53
6	Ozone dynamics and snowâ€ <b>e</b> tmosphere exchanges during ozone depletion events at Barrow, Alaska. Journal of Geophysical Research, 2012, 117, .	3.3	52
7	Intercomparison of NO <sub>2</sub> , O <sub>4</sub> , O <sub>3</sub> and HCHO slant column measurements by MAX-DOAS and zenith-sky UV–visible spectrometers during CINDI-2. Atmospheric Measurement Techniques, 2020, 13, 2169-2208.	3.1	52
8	Observations of bromine monoxide transport in the Arctic sustained on aerosol particles. Atmospheric Chemistry and Physics, 2017, 17, 7567-7579.	4.9	44
9	Atmospheric mercury over sea ice during the OASIS-2009 campaign. Atmospheric Chemistry and Physics, 2013, 13, 7007-7021.	4.9	42
10	Dependence of the vertical distribution of bromine monoxide in the lower troposphere on meteorological factors such as wind speed and stability. Atmospheric Chemistry and Physics, 2015, 15, 2119-2137.	4.9	41
11	Glyoxal observations in the global marine boundary layer. Journal of Geophysical Research D: Atmospheres, 2014, 119, 6160-6169.	3.3	38
12	Detection of water vapour absorption around 363†nm in measured atmospheric absorption spectra and its effect on DOAS evaluations. Atmospheric Chemistry and Physics, 2017, 17, 1271-1295.	4.9	36
13	Daytime HONO, NO <sub>2</sub> and aerosol distributions from MAX-DOAS observations in Melbourne. Atmospheric Chemistry and Physics, 2018, 18, 13969-13985.	4.9	34
14	Intercomparison of MAX-DOAS vertical profile retrieval algorithms: studies using synthetic data. Atmospheric Measurement Techniques, 2019, 12, 2155-2181.	3.1	34
15	The Heidelberg Airborne Imaging DOAS Instrument (HAIDI) – a novel imaging DOAS device for 2-D and 3-D imaging of trace gases and aerosols. Atmospheric Measurement Techniques, 2014, 7, 3459-3485.	3.1	33
16	Intercomparison of MAX-DOAS vertical profile retrieval algorithms: studies on field data from the CINDI-2 campaign. Atmospheric Measurement Techniques, 2021, 14, 1-35.	3.1	32
17	Validation of tropospheric NO <sub>2</sub> column measurements of GOME-2A and OMI using MAX-DOAS and direct sun network observations. Atmospheric Measurement Techniques, 2020, 13, 6141-6174.	3.1	31
18	On the relative absorption strengths of water vapour in the blue wavelength range. Atmospheric Measurement Techniques, 2015, 8, 4329-4346.	3.1	30

Udo Frieß

#	Article	IF	CITATIONS
19	MAX-DOAS retrieval of aerosol extinction properties in Madrid, Spain. Atmospheric Measurement Techniques, 2016, 9, 5089-5101.	3.1	30
20	The impact of vibrational Raman scattering of air on DOAS measurements of atmospheric trace gases. Atmospheric Measurement Techniques, 2015, 8, 3767-3787.	3.1	27
21	Horizontal and vertical structure of reactive bromine events probed by bromine monoxide MAX-DOAS. Atmospheric Chemistry and Physics, 2017, 17, 9291-9309.	4.9	27
22	Biogenic halocarbons from the Peruvian upwelling region as tropospheric halogen source. Atmospheric Chemistry and Physics, 2016, 16, 12219-12237.	4.9	22
23	Springtime Bromine Activation over Coastal and Inland Arctic Snowpacks. ACS Earth and Space Chemistry, 2018, 2, 1075-1086.	2.7	22
24	Is a scaling factor required to obtain closure between measured and modelled atmospheric O <sub>4</sub> absorptions? An assessment of uncertainties of measurements and radiative transfer simulations for 2 selected days during the MAD-CAT campaign. Atmospheric Measurement Techniques, 2019, 12, 2745-2817.	3.1	22
25	Inter-comparison of MAX-DOAS measurements of tropospheric HONO slant column densities and vertical profiles during the CINDI-2 campaign. Atmospheric Measurement Techniques, 2020, 13, 5087-5116.	3.1	18
26	Vertical distribution of BrO in the boundary layer at the Dead Sea. Environmental Chemistry, 2015, 12, 438.	1.5	16
27	Time-dependent 3D simulations of tropospheric ozone depletion events in the Arctic spring using the Weather Research and Forecasting model coupled with Chemistry (WRF-Chem). Atmospheric Chemistry and Physics, 2021, 21, 7611-7638.	4.9	13
28	Evaluating different methods for elevation calibration of MAX-DOAS (Multi AXis Differential Optical) Tj ETQq0 0 C Techniques, 2020, 13, 685-712.	) rgBT /Ον 3.1	erlock 10 Tf 11
29	CARIBIC DOAS observations of nitrous acid and formaldehyde in a large convective cloud. Atmospheric Chemistry and Physics, 2014, 14, 6621-6642.	4.9	8
30	Detection of O <sub>4</sub> absorption around 328 and 419 nm in measured atmospheric absorption spectra. Atmospheric Chemistry and Physics, 2018, 18, 1671-1683.	4.9	7
31	Recent improvements of long-path DOAS measurements: impact on accuracy and stability of short-term and automated long-term observations. Atmospheric Measurement Techniques, 2019, 12, 4149-4169.	3.1	7
32	The role of open lead interactions in atmospheric ozone variability between Arctic coastal and inland sites. Elementa, 2016, 4, .	3.2	6
33	Validation of MAX-DOAS retrievals of aerosol extinction, SO <sub>2</sub> , and NO <sub>2</sub> through comparison with lidar, sun photometer, active DOAS, and aircraft measurements in the Athabasca oil sands region. Atmospheric Measurement Techniques, 2020, 13, 1129-1155.	3.1	4
34	Evolution of observed ozone, trace gases, and meteorological variables over Arrival Heights, Antarctica (77.8°S, 166.7°E) during the 2019 Antarctic stratospheric sudden warming. Tellus, Series B: Chemical and Physical Meteorology, 2022, 73, 1933783.	1.6	3
35	Retrieval algorithm for OClO from TROPOMI (TROPOspheric Monitoring Instrument) by differential optical absorption spectroscopy. Atmospheric Measurement Techniques, 2021, 14, 7595-7625.	3.1	2
36	Enhancing MAX-DOAS atmospheric state retrievals by multispectral polarimetry – studies using synthetic data. Atmospheric Measurement Techniques, 2022, 15, 2077-2098.	3.1	2

#	Article	IF	CITATIONS
37	Ground-based validation of the MetOp-A and MetOp-B GOME-2 OClO measurements. Atmospheric Measurement Techniques, 2022, 15, 3439-3463.	3.1	0